Ultrasonics Sonochemistry 83 (2022) 105936

Contents lists available at ScienceDirect

Ultrasonics Sonochemistry

journal homepage: www.elsevier.com/locate/ultson

A Lotus shaped acoustofluidic mixer: High throughput homogenisation of liquids in 2 ms using hydrodynamically coupled resonators

Amir Pourabed [a], Jason Brenker [a], Tayyaba Younas [b], Lizhong He [b], Tuncay Alan [a,*]

[a] Department of Mechanical and Aerospace Engineering, Monash University, Melbourne, Australia
[b] Department of Chemical Engineering, Monash University, Melbourne, Australia

ARTICLE INFO

Keywords:
Acoustic microfluidic mixer
Coupled resonators
Mixing
PLGA nanoparticles

ABSTRACT

This paper presents an acoustically actuated microfluidic mixer that uses an array of hydrodynamically coupled resonators to rapidly homogenise liquid solutions and synthesise nanoparticles. The system relies on 8 identical oscillating cantilevers that are equally spaced on the perimeter of a circular well, through which the liquid solutions are introduced. When an oscillatory electrical signal is applied to a piezoelectric transducer attached to the device, the cantilevers start resonating. Due to the close proximity between the cantilevers, their circular arrangement and the liquid medium in which they are immersed, the vibration of each cantilever affects the response of its neighbours. The streaming fields and shearing rates resulting from the oscillating structures were characterised. It was shown that the system can be used to effectively mix fluids at flow rates up to 1400 $\mu l.min^{-1}$ in time scales as low as 2 ms. The rapid mixing time is especially advantageous for nanoparticle synthesis, which is demonstrated by synthesising Poly lactide-co-glycolic acid (PLGA) nanoparticles with 52.2 nm size and PDI of 0.44.

1. Introduction

Rapid and effective mixing of reacting chemicals in controlled time scales is crucial for the synthesis of new materials [1,2], studying and tuning nucleation events [3] as well as assembly of organic and inorganic nanoparticles with uniform size and size distribution [4]. Controlling the efficiency and time of mixing is not a simple task using conventional batch methods, where the concentrations of reacting solutions fluctuate over a few seconds before the mixture fully homogenises [5], which may result in inhomogeneity of products for reactions with a fast kinetics. Acoustically actuated microfluidic systems offer unique advantages to mix sample volumes at stable concentrations, and varying times. Both of these can be employed to tune the morphology and size of the generated particles, which in turn control their functionality [4].

Acoustically actuated mixers commonly rely on acoustic streaming, the attenuation of propagated sound wave within viscous fluid, as the main mechanism to enhance mixing. Generally, acoustic streaming within microfluidics is generated by either surface acoustic waves (SAWs) or bulk acoustic waves (BAWs) [6,7]. In SAW devices, a sound wave travelling on the surface of the substrate, along the interface of the fluid with the substrate, interacts with the fluid medium, exerting a body force which generates a streaming velocity. In BAW devices the wave travelling along the thickness of the substrate scatters into the fluid medium. Although SAW devices benefit from better control over actuation frequency, BAW microfluidics provides advantages such as higher throughput, facile and cost effective fabrication [6,8]. In micron scale, when an oscillating structure is in contact with fluid, the viscous dissipation in the viscous boundary layer is the main mechanism driving acoustic streaming in the bulk of fluid. This is due to no slip boundary condition between solid and fluid generating a velocity gradient in viscous layer, which is known as boundary driven acoustic streaming. Further, the boundary layer streaming induces a streaming within bulk of the fluid named outer streaming or bulk streaming i.e. observable streaming [9]. This concept has been successfully used to fabricate acoustic microfluidic mixers with efficient mixing within millisecond ranges [10–12].

It has been shown that oscillating sharp edge cantilevers can be used effectively to generate acoustic streaming within microfluidic channel by introducing discontinuities at the tip of the vibrating cantilevers [13,14]. A thorough numerical analysis on sharp edge geometry and its effect on the strength of acoustic streaming is covered widely [15,16]. It

* Corresponding author.
E-mail address: tuncay.alan@monash.edu (T. Alan).

https://doi.org/10.1016/j.ultsonch.2022.105936
Received 29 September 2021; Received in revised form 10 January 2022; Accepted 26 January 2022
Available online 31 January 2022
1350-4177/© 2022 The Author(s). Published by Elsevier B.V. This is an open access article under the CC BY-NC-ND license (http://creativecommons.org/licenses/by-nc-nd/4.0/).

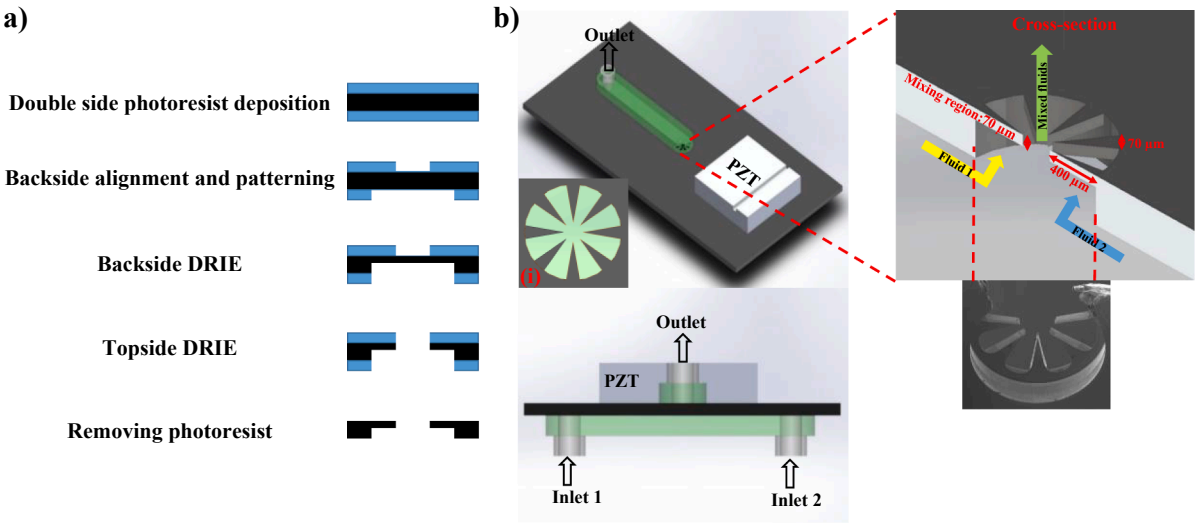

Fig. 1. a) Device fabrication process and b) schematic of the assembled device. (i) Top view of Lotus shaped structure.

is presented that cantilevers with sharper tips are more desirable since these can generate larger acoustic streaming thus better performance for intended applications [13]. In recent years, acoustic microfluidic devices based on sharp edged PDMS structures, bottom and top sides of which are fixed to the channel base and ceiling have been demonstrated for different applications such as cell lysis [17], pumping [18] and mixing [13] with remarkably improved performance.

Despite their impressive efficiency and speed, acoustically actuated microfluidic mixers are typically limited to low throughput (low $\mu l.min^{-1}$ range) operation. To maintain the efficiency at increased flow rates, the acoustic disturbance must be substantially improved, so that the mixing remains acoustic rather than advection dominated.

Varying flow rate operation can be accomplished by integrating acoustically oscillating structures with passive Tesla structures [19]. Additionally, combination of both oscillating sharp edges and micro bubbles [20] have also shown to be an effective methods in increasing throughput to $ml.min^{-1}$ ranges. However, the low elastic modulus and high damping materials (such as PDMS) used in some of the earlier approaches continue to limit the full dynamic potential of such oscillators, which in turn, compromise their throughput and mixing time. Increasing the stiffness and actuation frequency of the oscillators while maintaining a sufficient displacement amplitude could potentially improve the disturbance further even at significantly higher flow rates.

To demonstrate this potential, we have recently embedded resonators made of stiffer structures made of high elastic modulus materials such as silicon nitride (SiN) and Silicon (Si) [14,21]. These devices can operate at higher frequencies compared to other acoustically activated devices. In all of these cases, implementation of free-standing oscillatory structures with high actuation frequency introduces stronger body forces in the fluid medium and stronger acoustic streaming [14,21]. It has been shown that these devices were able to operate at flow rates approaching 8 $ml.min^{-1}$ providing a 4-fold improvement in throughput over similar approaches [14,21,22]. These devices were successfully demonstrated in self-assembly of different nanoparticles [14,21,22].

Here, we show that the mixing time could be further reduced; the device fabrication could be simplified and made more robust while maintaining a sufficiently high throughput operation. We propose a Lotus shaped acoustic mixer containing eight freestanding silicon-based sharp edge oscillators actuated at their resonant frequency. Essentially, the nature of freestanding oscillators gives more flexibility in their vibration amplitude and the silicon oscillators provide a stronger body force thus generating stronger acoustic streaming in comparison to its PDMS oscillating counterparts. Due to its unique fabrication method, the device could be produced by precisely controlling the oscillating geometry, therefore it offers better control on actuation frequency. Additionally, confining the sharp edges within a circular boundary shrinks the effective mixing length to the thickness of the oscillators. Taking advantage of these features, the mixing time is reduced by up to 6-fold compared to our previous mixer and maintain operating flow rates up to 1400 $\mu l.min^{-1}$ with mixing efficiency of 90%. As a proof of concept, the Lotus shaped mixer was employed for the self-assembly of poly (lactide-co-glycolic acid) (PLGA) nanoparticles. PLGA is a biodegradable polymer and is widely used as carrier in drug delivery applications. The device was capable of producing nanoparticles with size and PDI of 52 nm and 0.44, respectively.

2. Methodology and characterisation

2.1. Device fabrication and assembly

Fig. 1a shows the fabrication process for the device, which contains freestanding oscillating sharp edge cantilevers sandwiched between two PDMS channels. Two inlets from the bottom channel are used to deliver the fluids to the central mixing region. The homogenised fluid exits from the top channel. Double side deep reactive ion etching (DRIE) was implemented to fabricate the freestanding cantilevers. SU-8 3025 was coated on both sides of a 300 µm thick double-sided polished Si wafer (100-orientation). A standard photolithography procedure (EVG 6200 mask aligner) was used to pattern the cantilever features on the top side of the Si wafer. Next, 1-mm-diameter circular wells were produced on the backside of the wafer. The Lotus root pattern contains eight triangular cantilevers the base width and length of which are 70 and 400 µm, respectively. DRIE process was used to etch the backside of the wafer to a depth of 230 µm and the topside was etched-through the wafer to release the freestanding cantilevers with thickness of 70 µm. The devices were then diced, sandwiched between two PDMS channels, and a 1-mm thick ceramic piezoelectric (PZT) disk (PZ26 Maggit pty) was attached on each chip using epoxy glue (Fig. 1b). In the experiments, the PZT was actuated using Standford Research System DS345 signal generator and the output signals were amplified by T&C power conversion, INC. AG 1006 amplifier at 0.1% gain.

2.2. Simulation

Comsol Multiphysics v5.1 was used to study frequency response of single cantilever in 3D mode by applying a body load on the cantilever following a frequency sweep within 500–1500 kHz range with an increment of 10 kHz. Later, the maximum frequency response as result

Table 1
Parameters of the finite element analysis (FEA).

Parameter	Symbol	Unit	Value
Fluid Water			
Density	ρ_f	$Kg.m^{-3}$	1000
Speed of sound	C_f	$m.s^{-1}$	1500
Frequency	f	MHz	0.79
Viscous boundary layer	ν	nm	585
Maximum mesh size	e_f	μm	5.85
Curvature factor	–	–	0.2
Mesh growth factor	–	–	1.08
Solid			
Silicon (Solid ⟨1 0 0⟩)			
Mesh size (General Physics: Finer)			
Fluid-Solid boundary layer			
Number of layers: 3			
Boundary stretching factor: 1.2			
Thickness of layer: 195 nm			

of the in-plane mode of vibration was used as an input to study hydrodynamic effect of solid structures and its corresponding streaming velocity exerted on the fluid (water in this study). A 2D Thermoviscous Acoustic-Solid Interaction study was used for this purpose. The study was performed by applying a body load on the whole Lotus shaped structure at the frequency corresponding to in-plane vibrational mode of cantilevers. In order to avoid singularity effects, the cantilevers' tip were rounded to a 1 μm radius. Table 1 presents the parameters considered for the FEA analysis. The minimum and maximum mesh sizes were chosen based on earlier work [14,21]. Considering viscous boundary layer thickness (ν), the minimum mesh size was selected as ($\nu/3$) at fluid–solid boundary with maximum mesh size of ($10^*\nu$) in the fluid domain in order to minimise computational memory.

2.3. Characterisation

2.3.1. Scanning electron microscopy (SEM)

FEI Nova NanoSEM 430 Instrument was used to characterise cross-section and the length of cantilevers after fabrication. The images were captured at current of 56 pA and voltage of 5 kV.

2.3.2. Estimating the resonant frequency of the device

Polytec MSA-400 LDV employed to measure the resonant frequency of sharp edge cantilevers (out of plane mode). The mode of measurement was set on periodic chirp within 500–1500 kHz range at the region of interest (scanning mode). In addition, 6 μm fluorescent tagged polystyrene particles (Duke Scientific Corp. Palo Alto) were used to visualise the acoustic streaming generated by vibration of cantilevers. Frequency sweep performed at zero flow rate within 500–1500 kHz with 10 kHz step size (0.65–3.33 W power input) and the particle behaviour were recorded by Nikon upright microscope equipped with a camera. The resonant frequency was found at 680 kHz as the device generates strongest streaming at this frequency. Furthermore, Comsol multiphysics 5.1 was used to numerically estimate the in-plane mode of vibration and hydrodynamic effect of cantilevers on the streaming velocity and their oscillating behaviour. The methodology for the simulation adopted from the ref [21].

2.3.3. High speed videography

HX6 high-speed digital camera (Model number: ST-826) used to monitor velocity of polystyrene particles (diameter: 6 μm) around each individual cantilever. Recordings were made at 41,190 frames per second, frame size of 320*280 pixels (2 μm/Pixel), shutter speed of 24.1 μs and pixel bit depth of 12. The mean particle velocity in the horizontal plane around each tip was analysed with droplet morphometry and velocimetry (DMV) software [23]. A total of 1750 frames were examined to measure average particle velocity for the whole structure and particle trajectories as well as pathlines were post processed via MATLAB using raw data extracted from DMV.

2.3.4. Mixing efficiency

Mixing efficiency was measured by mixing fluorescent dye and water at different flow rates and calculating relative mixing index (RMI) adopted from ref [21] in the region of interest (ROI). The relative mixing index, RMI was calculated by:

$$RMI = 1 - \sigma/\sigma_{0,}$$

where σ and σ_0 are the standard deviations of pixel intensity in mixed and unmixed region of interest and are obtained by:

$$\sigma = \sqrt{\frac{1}{N}\sum_{i=1}^{N}(I_i - < I >)^2}$$

$$\sigma_0 = \sqrt{\frac{1}{N}\sum_{i=1}^{N}(I_{oi} - < I >)^2}$$

N is the number of pixels, I_i, $<I>$ and I_{oi} are the local pixel intensity of the mixture, average intensity of the region of interest and local pixel intensity in unmixed mode respectively.

2.3.5. PLGA nanoparticle assembly and size characterisation

Initially, 1 $mg.ml^{-1}$ PLGA solution in Acetone was prepared. The PLGA nanoparticles were formed as result of nucleation and growth during the super saturation process by mixing PLGA solution (solvent) and water (anti-solvent) via Lotus shaped acoustofluidic mixer at flow rate and flow rate ratio of 1 $ml.min^{-1}$ and 1:1, respectively. Further, the size of particles was characterised using dynamic light scattering (DLS)

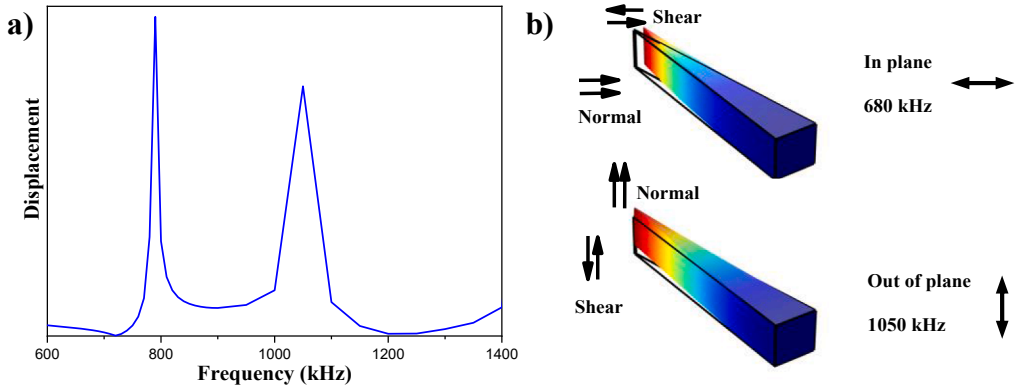

Fig. 2. a) FEA analysis of cantilever's frequency response. b) Direction of shear and normal forces on the cantilevers with respect to mode of vibration.

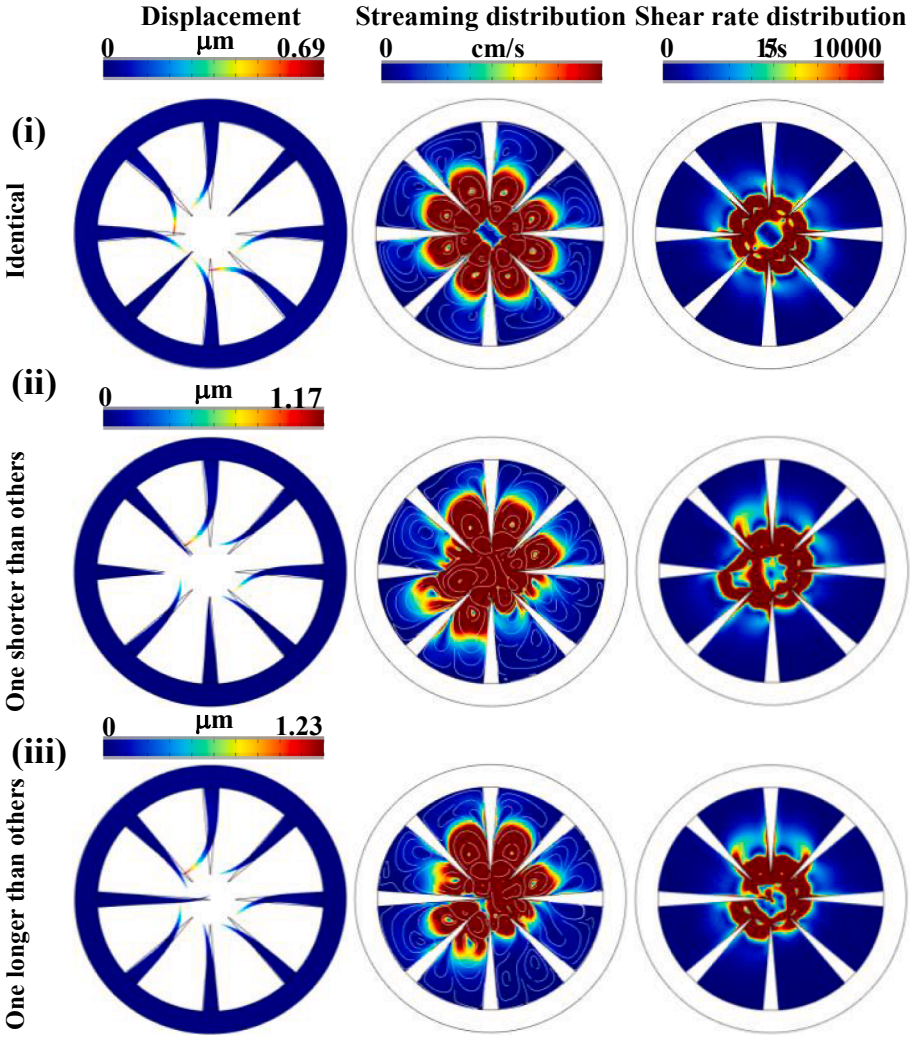

Fig. 3. Hydrodynamic effect on cantilevers displacement, streaming velocity and shear rate distribution in different scenarios: (i) all cantilevers are identical, (ii) one cantilever is shorter and (iii) one cantilever is longer than the rest. Note: The simulation was done under zero flow rate.

and transmission electron microscopy (TEM). For DLS analysis, three replicates were prepared and for each sample three measurements each comprising 10 cycles were performed using Zetasizer Nano ZS and size distribution of the particles were analysed using intensity percentage. TEM images were collected using FEI Tecnai G2 T20 TWIN LaB6, at 200 kV accelerating voltage. Six independent images were analysed using imageJ software. The poldydispersity of the sample was calculated with a total counting of 68 particles using Gaussian fit by Origin pro software.

3. Results and discussion

3.1. Simulations of the dynamic behaviour

The mixing within Lotus shaped mixer occurs as a result of acoustic streaming within the bulk of fluids [14,21,22,24]. When a high frequency alternating current is applied to a piezoelectric transducer attached to the device, the cantilevers start oscillating. This, in turn, perturbs the laminarly flowing fluid media surrounding them generating extremely high fluid particle velocities as discussed in section 3.2. The vibrational properties of the cantilevers and the coupling between them play a significant role in the strength of the streaming within the fluid medium. Thus, it is necessary to determine the actuation parameters.

To determine the optimum actuation parameters, the eigen-frequencies of the cantilevers were estimated with a finite element analysis (FEA) (Fig. 2a). Accordingly, the first two resonant modes of each cantilever occur at 790 kHz and 1050 kHz corresponding to in-plane and out-of-plane modes, respectively (the out of plane mode was confirmed with a Laser Doppler Vibrometer scan). For the present device configuration (Fig. 2b), it is hypothesised that when the out of plane mode is actuated, the streaming will not be significant due to the combined effect of the cantilever geometry and the backpressure exerted by the fluid flow [25]. In contrast, the in-plane vibrational mode (perpendicular to the flow direction) and the shearing forces resulting from it have the potential to drastically perturb the flow profiles and rapidly mix and homogenises liquids.

As a next step, considering only the (in-plane) 1st mode of vibration (Fig. 3), the dynamic behaviour of the resonating cantilevers embedded in the fluid medium and the corresponding streaming patterns through 2D FEA simulations were studied. Here, three different scenarios were taken into account: (i) all 8 cantilevers are identical; (ii) one cantilever is shorter than the others, and finally, (iii) one cantilever is longer than the others. The latter two cases were considered to take into account any slight geometric variations, which may occur due to the lithography process. Since the cantilevers are hydro-dynamically coupled, any slight variation could in turn affect the collective resonant frequency or vibrational phase.

The entire structure was vibrated at 790 kHz and the displacement of the cantilevers, the corresponding streaming velocities and shear rate distributions were calculated for all three cases. When all cantilevers are identical in length, they are oscillating in phase. The motion of each

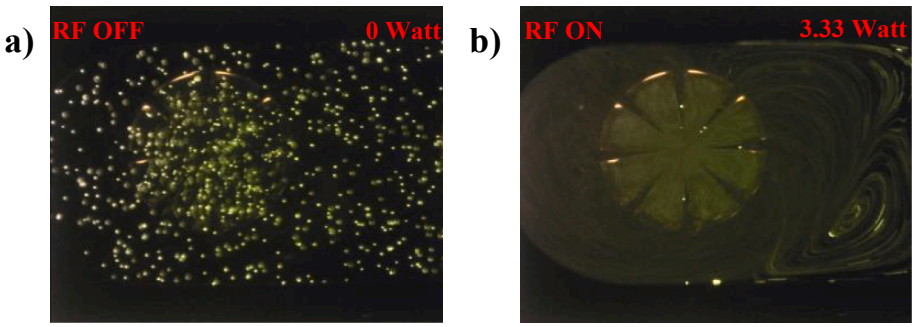

Fig. 4. Streaming patterns at 680 kHz under no flow rate; a) before and b) after actuation.

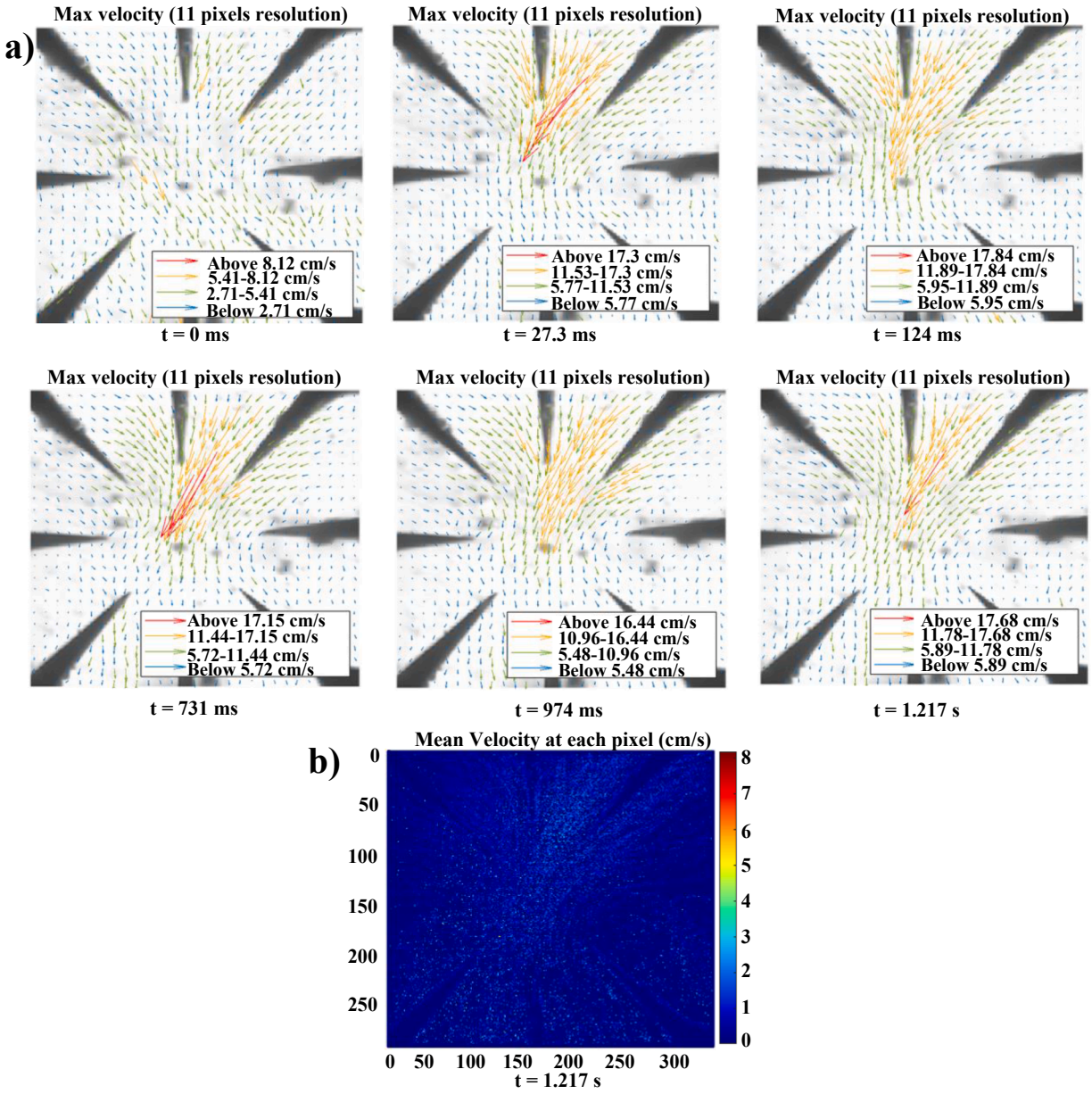

Fig. 5. a) Maximum particle velocity distribution at different time intervals. b) Mean particle velocity distribution at 1.217 s. (Experiments performed at zero flow rate).

cantilever pushes the fluid towards its neighbour, and exerts pressure on it. This results in a higher hydrodynamic dissipation, and reduces the cantilever displacement [26]. As a result, this case resulted in a relatively smaller vibration amplitude (Fig. 3i) than the other two scenarios. On the other hand, the synchronicity is compromised once the length of a single cantilever is varied (Fig. 3ii and iii), leading to less

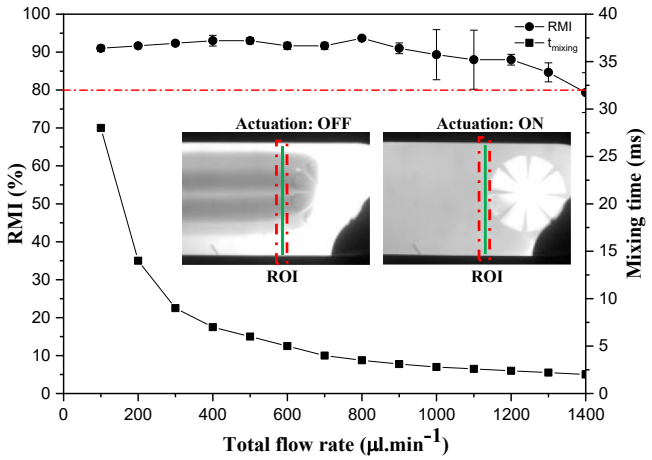

Fig. 6. RMI values and mixing time as a function of total flow rate (Inset image presents region of interest (ROI) where mixing efficiency is calculated).

added mass on adjacent cantilevers, and therefore, less hydrodynamic dissipation. While this does not dramatically change the maximum velocities and shear rates observed within fluid medium, the simulation results indicate that larger displacement amplitudes are observed for cases (ii) and (iii) with the latter resulting in maximum displacement. The larger displacements can be attributed to the extension of maximum velocity and shear rate distribution within fluid medium (i.e., larger fluid medium experiencing maximum velocity and shear rate). It was also noted that geometric irregularities may result in nonlinear modes, especially when the coupling between the cantilevers gets stronger (i.e., when the space between neighbouring cantilevers is reduced).

Therefore, based on aforementioned results, it could be suggested that in order to have a stronger streaming, it is desirable to minimise the coupling effect between oscillating cantilevers with appropriate proximity that provide enough synergic effect in efficient fluid perturbation [27].

3.2. Experimental analysis

Next, the assembled device comprising of 8 cantilevers immersed in a liquid medium was tested with fluorescent polystyrene (PS) particles and the streaming generated within the 500–1500 kHz actuation frequency range was visualised. As hypothesised above, the streaming behaviour was only observed at an actuation frequency of 680 kHz, close to the calculated 1st (in-plane) resonant frequency. (Fig. 4 and supplementary video S1). It is noted that the optimum experimental actuation frequency is smaller than the simulated value potentially due to the effects of liquid damping and interaction between adjacent cantilevers.

To estimate the streaming velocities, the particle trajectories at zero flow rate within the device through high-speed videography was analysed. As shown in supplementary video S2, upon acoustic actuation, particles are pushed towards the tip of each cantilever (where the maximum streaming velocity is observed) and accelerated towards the centre of the circular region. Fig. 5a shows the streaming velocities at different time intervals measured by MATLAB using DMV results. The device can achieve maximum particle velocities exceeding 17 cm.s^{-1}. The observed result is 5, 10 and 100 times higher than similar devices containing sharp edge structures, SAW based devices and similar bulk acoustic microfluidic mixers [17,28,29]. The maximum velocities are observed near cantilever tips and help pushing particles towards the

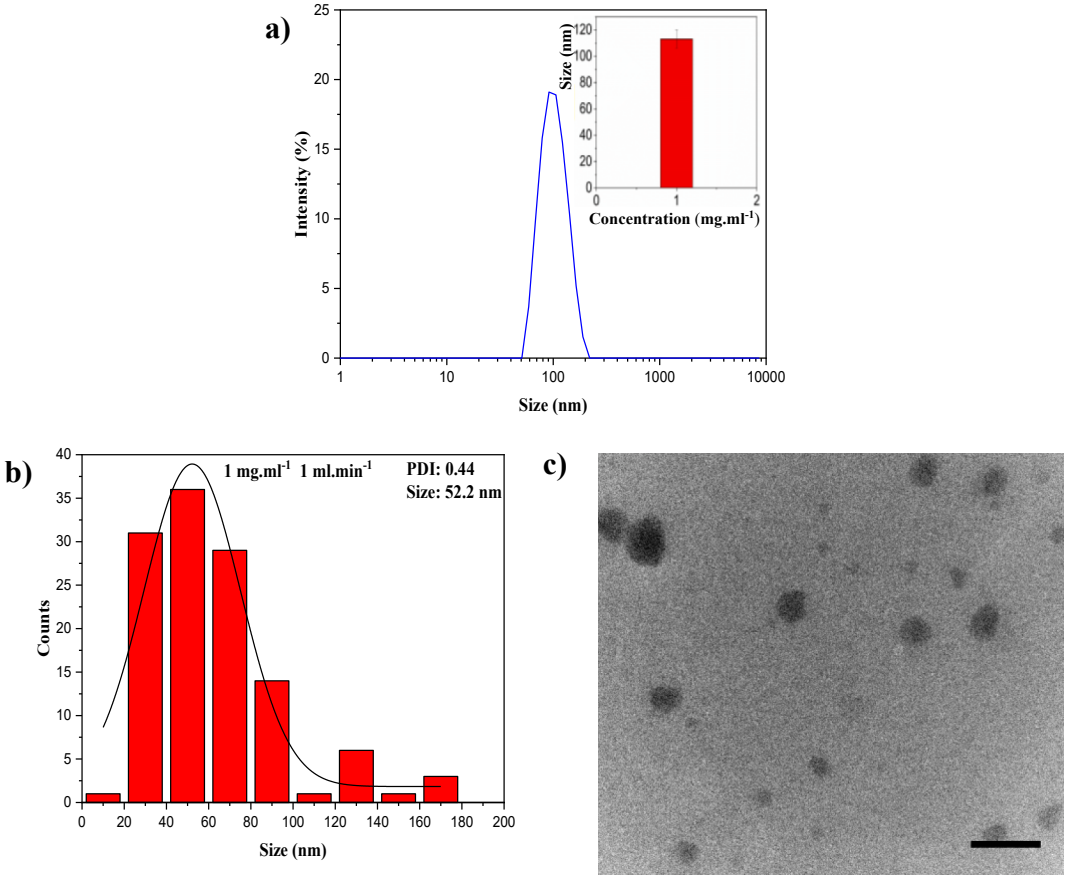

Fig. 7. a) DLS results of PLGA nanoparticles prepared at 1 mg.ml^{-1} concentration and flow rate of 1 ml.min^{-1}. Inset image presents the average particle size from three replicates. b) and c) with respect, size distribution and TEM image of PLGA particles (scale bar: 150 nm).

center of the circular mixing region. Fig. 5b shows the mean velocity distribution of particles at six time points covering the first 1.2 s after actuation.

The maximum velocities observed in the upper right quarter are consistently above 17 cm.s^{-1}, throughout the recorded frames, highlighting the stability of uniform fluid perturbation. On the opposite side, the maximum velocities at the bottom left region remain smaller than 5 cm.s^{-1}. It is hypothesised that this spatial variation in velocity between different regions could be due to slight differences in the cantilever geometries caused by the fabrication process. This is in agreement with streaming velocity distributions from simulation results scenarios (ii) and (iii). Particle velocities at all regions are considerably higher than what was observed by earlier approaches. Due to their high Young's modulus and mechanical stiffness, the silicon cantilevers operate in higher actuation frequencies compared to similar devices made of PDMS. This exerts higher body force into the fluid medium leading to stronger streaming velocities. Based on these high velocities and their spatial variation within the circular region, the device has a significant potential to enhance mixing within micron size channels at very fast time scales.

3.3. Application as a mixer

3.3.1. Mixing efficiency and mixing time

The capability of the device as an acoustic micro mixer was examined. Fig. 6 presents the region of interest (ROI), the mixing efficiency and mixing time with respect to total flow rate. The device was capable of mixing fluids at a 94% efficiency and a 1400 μl.min^{-1} flow rate. The Lotus shaped acoustic device can be easily operated at higher flow rates without needing additional passive components, a strategy used in some earlier designs to improve throughput [19]. It is noted that the Lotus design has unique advantages. The device employs 8 free-standing Si cantilevers positioned around the perimeter of a circular well. Si cantilevers have a higher stiffness, and, as importantly, a smaller damping coefficient than their elastomeric counterparts. The former ensures higher body forces can be imparted into the fluid, hence generating a stronger streaming field, the latter contributes to higher flowrate operation as it overcomes the backflow pressure more efficiently. As two liquids are passing through the well, all of the 8 cantilevers vibrate at the same time, at high amplitudes, in a plane perpendicular to the flow direction. Hence the vibration of each cantilever contributes to perturbing the fluid flow [14,22] resulting in a more effective mixing of fluid particles in shorter time scales. However, as the backflow pressure increases i.e. higher flow rate, it dominates the resonators' stiffness resulting drop in acoustic streaming strength. In Lotus shaped acoustofluidic device, the resonators stiffness could withhold backflow pressures up to 1400 μl. min-1 without compromising the mixing performance. As the flowrates are increased substantially, the mixing efficiency is expected to drop.

Another factor contributing to faster mixing (6- fold improvement over our previous higher throughput acoustic mixer) is the reduction of the mixing length from 500 to 70 μm in this design [22]. Complete mixing is achieved as the fluids travel through the cantilever thickness (l = 70 μm), which is substantially shorter than earlier devices. (The mixing time is estimated by $t_{mix} = \frac{l}{u}$ where l and u are the mixing length and average fluid velocity, respectively.) At a flowrate of 1400 μl.min^{-1}, two liquids can be mixed in 2 ms with an efficiency of 80% while the maximum observed efficiency is 94%. As the flowrate increases to 1400 μl.min^{-1}, the higher back flow pressure dominates the cantilevers' damping coefficient, which reduced the mixing efficiency to 80%.

3.3.2. PLGA self-assembly

As proof of concept, the Lotus shaped acoustic device was deployed for self-assembly of PLGA nanoparticles. Fig. 7a shows the size distribution of PLGA nanoparticles measured by DLS with an average hydrodynamic diameter of 113 nm. The TEM images (Fig. 7b and c) showed formation of particles with average size of 52.2 nm and PDI 0.44. Super saturation rate (the rate of uniform mixing between solvent and anti-solvent) and the concentration gradients across the solutions play a crucial role in the formation of nanoparticles with a narrow size distribution. Further reducing the mixing time beyond what is reported here without compromising the mixing efficiency will potentially lower the concentration gradient across the solutions providing identical growth rates for each nucleation site and hence result in a narrower size distribution.

Depending on the chemical system being considered, it is anticipated that geometric modifications to the Lotus mixer can be used to tune the particle uniformity. For instance increasing the number of cantilevers would lead to reducing the surface area where fluids are mixed as they pass the mixing section, which essentially reduces the mixing time. This increases the rate of super saturation as well as the nucleation sites resulting in nanoparticles with smaller size. Similarly, changes in the cantilever geometry can be used to enhance the mixing strength.

4. Conclusion

This paper introduces a Lotus shaped acoustic micro-mixer that can be actuated at high frequencies with mixing efficiencies as high as 94%. The new design enables the actuation frequency, stiffness of oscillating sharp edges as well as mixing time to be easily tuned for the specific applications. The simulations and experimental results showed that effective fluid perturbation can be achieved when mode of oscillation induces shear forces within bulk of medium (in-plane mode in this study) and hydrodynamic coupling between oscillators are minimised. Further, monitoring particle velocities resulting from acoustic streaming via high speed videography analysis showed that the device is capable of inducing fast perturbation within fluid medium reaching a maximum particle velocity of 17 cm.s^{-1}. Compared to our previously reported device, we were able to improve mixing time by 6 fold at a given flow rate via reducing mixing length while maintaining the mixing efficiency achieving a minimum mixing time of 2 ms with a maximum operating flow rate of 1400 μl.min^{-1}. Using Lotus shaped acoustofluidic device, PLGA nanoparticles as small as 52 nm were assembled. The potential use of this device is not limited to mixing only but also for various applications such as sonoporation [30], cell lysis [31] and kinetics measurements [10,32].

CRediT authorship contribution statement

Amir Pourabed: Conceptualization, Methodology, Investigation, Resources, Validation, Data curation, Formal analysis, Writing – original draft. **Jason Brenker:** Resources, Validation, Writing – review & editing. **Tayyaba Younas:** Resources, Writing – review & editing. **Lizhong He:** Supervision, Writing – review & editing. **Tuncay Alan:** Supervision, Writing – review & editing.

Declaration of Competing Interest

The authors declare that they have no known competing financial interests or personal relationships that could have appeared to influence the work reported in this paper.

Acknowledgement

This work was performed in part at the Melbourne Centre for Nanofabrication (MCN) in the Victorian Node of the Australian National Fabrication Facility (ANFF). We acknowledge Monash Centre for Electron Microscopy for access of TEM facility. This work was funded by NHMRC Development Grant 2000120 .

Appendix A. Supplementary data

Supplementary data to this article can be found online at https://doi.org/10.1016/j.ultsonch.2022.105936.

References

[1] C.-T. Kung, et al., Microfluidic synthesis control technology and its application in drug delivery, bioimaging, biosensing, environmental analysis and cell analysis, Chemical Engineering Journal 399 (2020), 125748.

[2] M. Ni, G. Tresset, C. Iliescu, Self-assembled polysulfone nanoparticles using microfluidic chip, Sensors and Actuators B: Chemical 252 (2017) 458–462.

[3] P. Coliaie, M.S. Kelkar, N.K. Nere, M.R. Singh, Continuous-flow, well-mixed, microfluidic crystallization device for screening of polymorphs, morphology, and crystallization kinetics at controlled supersaturation, Lab on a Chip 19 (14) (2019) 2373–2382.

[4] P.-H. Huang, S. Zhao, H. Bachman, N. Nama, Z. Li, C. Chen, S. Yang, M. Wu, S. P. Zhang, T.J. Huang, Acoustofluidic synthesis of particulate nanomaterials, Advanced Science 6 (19) (2019) 1900913, https://doi.org/10.1002/advs.v6.1910.1002/advs.201900913.

[5] P.M. Valencia, O.C. Farokhzad, R. Karnik, R. Langer, Microfluidic technologies for accelerating the clinical translation of nanoparticles, Nature nanotechnology 7 (10) (2012) 623–629.

[6] X. Ding, P. Li, S.-C. Lin, Z.S. Stratton, N. Nama, F. Guo, D. Slotcavage, X. Mao, J. Shi, F. Costanzo, T.J. Huang, Surface acoustic wave microfluidics, Lab on a Chip 13 (18) (2013) 3626, https://doi.org/10.1039/c3lc50361e.

[7] I. Leibacher, P. Reichert, J. Dual, Microfluidic droplet handling by bulk acoustic wave (BAW) acoustophoresis, Lab on a Chip 15 (13) (2015) 2896–2905.

[8] Y. Lin, C. Gao, Y. Gao, M. Wu, A. Ahmadian Yazdi, J. Xu, Acoustofluidic micromixer on lab-on-a-foil devices, Sensors and Actuators B: Chemical 287 (2019) 312–319.

[9] M. Wiklund, R. Green, M. Ohlin, Acoustofluidics 14: Applications of acoustic streaming in microfluidic devices, Lab on a Chip 12 (14) (2012) 2438–2451.

[10] X. Li, Z. He, C. Li, P. Li, One-Step Enzyme Kinetics Measurement in 3D Printed Microfluidics Devices based on A High-Performance Single Vibrating Sharp-Tip Mixer, Analytica Chimica Acta 1172 (2021) 338677, https://doi.org/10.1016/j.aca.2021.338677.

[11] P.-H. Huang, Y. Xie, D. Ahmed, J. Rufo, N. Nama, Y. Chen, C.Y. Chan, T.J. Huang, An acoustofluidic micromixer based on oscillating sidewall sharp-edges, Lab on a Chip 13 (19) (2013) 3847, https://doi.org/10.1039/c3lc50568e.

[12] C. Pothuri, M. Azharudeen, K. Subramani, Rapid mixing in microchannel using standing bulk acoustic waves, Physics of Fluids 31 (12) (2019) 122001, https://doi.org/10.1063/1.5126259.

[13] A.A. Doinikov, M.S. Gerlt, A. Pavlic, J. Dual, Acoustic streaming produced by sharp-edge structures in microfluidic devices, Microfluidics and Nanofluidics 24 (5) (2020), https://doi.org/10.1007/s10404-020-02335-5.

[14] N.H. An Le, H. Deng, C. Devendran, N. Akhtar, X. Ma, C. Pouton, H.-K. Chan, A. Neild, T. Alan, Ultrafast star-shaped acoustic micromixer for high throughput nanoparticle synthesis, Lab on a Chip 20 (3) (2020) 582–591.

[15] N. Nama, P.-H. Huang, T.J. Huang, F. Costanzo, Investigation of acoustic streaming patterns around oscillating sharp edges, Lab on a Chip 14 (15) (2014) 2824–2836.

[16] M. Ovchinnikov, J. Zhou, S. Yalamanchili, Acoustic streaming of a sharp edge, The Journal of the Acoustical Society of America 136 (1) (2014) 22–29.

[17] Z. Wang, P.-H. Huang, C. Chen, H. Bachman, S. Zhao, S. Yang, T.J. Huang, Cell lysis via acoustically oscillating sharp edges, Lab on a Chip 19 (24) (2019) 4021–4032.

[18] P.-H. Huang, N. Nama, Z. Mao, P. Li, J. Rufo, Y. Chen, Y. Xie, C.-H. Wei, L. Wang, T. J. Huang, A reliable and programmable acoustofluidic pump powered by oscillating sharp-edge structures, Lab on a Chip 14 (22) (2014) 4319–4323.

[19] H. Bachman, C. Chen, J. Rufo, S. Zhao, S. Yang, Z. Tian, N. Nama, P.-H. Huang, T. J. Huang, An acoustofluidic device for efficient mixing over a wide range of flow rates, Lab on a Chip 20 (7) (2020) 1238–1248.

[20] M.R. Rasouli, M. Tabrizian, An ultra-rapid acoustic micromixer for synthesis of organic nanoparticles, Lab on a Chip 19 (19) (2019) 3316–3325.

[21] H.V. Phan, M.B. Coşkun, M. Şeşen, G. Pandraud, A. Neild, T. Alan, Vibrating membrane with discontinuities for rapid and efficient microfluidic mixing, Lab on a Chip 15 (21) (2015) 4206–4216.

[22] A. Pourabed, T. Younas, C. Liu, B.K. Shanbhag, L. He, T. Alan, High throughput acoustic microfluidic mixer controls self-assembly of protein nanoparticles with tuneable sizes, Journal of Colloid and Interface Science 585 (2021) 229–236.

[23] A.S. Basu, Droplet morphometry and velocimetry (DMV): a video processing software for time-resolved, label-free tracking of droplet parameters, Lab on a Chip 13 (10) (2013) 1892–1901.

[24] N.H.A. Le, et al., Acoustically enhanced microfluidic mixer to synthesize highly uniform nanodrugs without the addition of stabilizers, International journal of nanomedicine 13 (2018) 1353.

[25] I. Dufour, et al., Effect of hydrodynamic force on microcantilever vibrations: Applications to liquid-phase chemical sensing, Sensors and Actuators B: Chemical 192 (2014) 664–672.

[26] S. Basak, A. Raman, Hydrodynamic coupling between micromechanical beams oscillating in viscous fluids, Physics of Fluids 19 (1) (2007) 017105, https://doi.org/10.1063/1.2423254.

[27] S. Zhao, P.-H. Huang, H. Zhang, J. Rich, H. Bachman, J. Ye, W. Zhang, C. Chen, Z. Xie, Z. Tian, P. Kang, H. Fu, T.J. Huang, Fabrication of tunable, high-molecular-weight polymeric nanoparticles via ultrafast acoustofluidic micromixing, Lab on a Chip 21 (12) (2021) 2453–2463.

[28] C. Westerhausen, L. Schnitzler, D. Wendel, R. Krzysztoń, U. Lächelt, E. Wagner, J. Rädler, A. Wixforth, Controllable acoustic mixing of fluids in microchannels for the fabrication of therapeutic nanoparticles, Micromachines 7 (9) (2016) 150, https://doi.org/10.3390/mi7090150.

[29] P. Gelin, Ö. Sardan Sukas, K. Hellemans, D. Maes, W. De Malsche, Study on the mixing and migration behavior of micron-size particles in acoustofluidics, Chemical Engineering Journal 369 (2019) 370–375.

[30] J.N. Belling, L.K. Heidenreich, Z. Tian, A.M. Mendoza, T.-T. Chiou, Y. Gong, N. Y. Chen, T.D. Young, N. Wattanatorn, J.H. Park, L. Scarabelli, N. Chiang, J. Takahashi, S.G. Young, A.Z. Stieg, S. De Oliveira, T.J. Huang, P.S. Weiss, S. J. Jonas, Acoustofluidic sonoporation for gene delivery to human hematopoietic stem and progenitor cells, Proceedings of the National Academy of Sciences 117 (20) (2020) 10976–10982.

[31] A.M. Kaba, H. Jeon, A. Park, K. Yi, S. Baek, A. Park, D. Kim, Cavitation-microstreaming-based Lysis and DNA Extraction using a Laser-machined Polycarbonate Microfluidic Chip, Sensors and Actuators B: Chemical 346 (2021) 130511, https://doi.org/10.1016/j.snb.2021.130511.

[32] M. Li, C. Dong, M.-K. Law, Y. Jia, P.-I. Mak, R.P. Martins, Hydrodynamic-flow-enhanced rapid mixer for isothermal DNA hybridization kinetics analysis on digital microfluidics platform, Sensors and Actuators B: Chemical 287 (2019) 390–397.